J. Materials, Conc. Struct., Pavements, JSCE, No.669/V-50, 309-321, 2001 February

EXPERIMENTAL STUDY ON PARAMETERS IN LOCALIZATION OF CONCRETE SUBJECTED TO COMPRESSION

Torsak LERTSRISAKULRAT[1], Ken WATANABE[2], Maki MATSUO[3] and Junichiro NIWA[4]

[1]Member of JSCE, Ms. Eng., Graduate Student, Dept. of Civil Eng., Tokyo Institute of Technology (2-12-1 O-okayama, Meguro-ku, Tokyo 152-8552, Japan)
[2]Member of JSCE, Graduate Student, Dept. of Civil Eng., Tokyo Institute of Technology
[3]Member of JSCE, Ms. Eng., Research Associate, Dept. of Civil Eng., Tokyo Institute of Technology
[4]Fellow of JSCE, Dr. Eng., Professor, Dept. of Civil Eng., Tokyo Institute of Technology

An experimental program has been conducted in order to examine the failure mechanism and localization effect of concrete subjected to uniaxial compression by measuring the distribution of local vertical strain inside a concrete specimen. The new quantitative approach of localized compressive fracture length has been presented. By considering the geometrical parameters and the properties of concrete used, it has been found that, when localization occurs, the localized compressive fracture length depends only on the size of the cross-section of the specimen. The new definition of fracture energy in compression in terms of externally applied energy per unit fracture volume has also been introduced.

Key Words: *fracture mechanics, localization, size effects, fracture energy in compression, localized compressive fracture length*

1. INTRODUCTION

It is now generally accepted that the failure of concrete in tension is localized to a limited zone. Many researchers have studied the localization behavior of concrete in tension and useful results have been obtained[1]. The localized behavior in tension is modeled by stress-crack width relationship based on the tensile fracture energy (G_F). A uniaxial description of the properties is sufficiently realistic, because no major lateral deformations take place simultaneously.

On the other hand, material models for compressive failure of concrete are normally based on a uniaxial compressive stress-strain curve obtained from tests, where the uniform deformation throughout a concrete specimen is assumed. This assumption is reasonable for the ascending branch of the stress-strain curve, but not necessarily accurate for the descending branch. As it was found that the deformation after the peak stress is localized to certain zones[2], so descending branch of the stress-strain curve becomes size dependent as the measured strain depends on the gage length and position of the gage[3]. Though many studies were carried out[4),5], the localization behavior and fracture zone of concrete in compression have not yet been clarified. The compressive failure is more complex than tensile failure, because it is always accompanied with significant lateral deformations. The lateral deformations are mainly caused by splitting cracks, which form and expand during the failure process. In addition to these cracks, localized shear bands may also form. Thus, the fracture process in compression is not only determined by localized cracks, as in tension, but in a realistic manner both the local and the continuum components of compressive softening have to be taken into account.

It is necessary to study the behaviors of concrete under compression by considering also the localization of cracks and fracture energy of concrete in compression, in order to be able to analyze the post-peak behavior of concrete in the more realistic

manner. Furthermore, the realistic stress-strain curve of concrete in uniaxial compression which takes into account the localization behavior will lead to more accurate results in the analysis of bending stresses in reinforced concrete members[6].

2. REVIEW OF PREVIOUS RESEARCH WORKS

The problem of finding the accurate localized compressive length has been discussed so far. Markeset and Hillerborg[5),7)] took the value of damaged zone, L^d, as 2.5 times the smallest lateral dimension of the concrete cross-section. The proposed value is based on the findings of other researchers[3),8)] that the compressive strength, f_c', of a specimen becomes constant when the slenderness ratio of that specimen reaches the value of about 2.5. In addition, the constant value of f_c' was obtained regardless of the technique of testing or end restrain conditions. However, there was no direct measurement of the fracture length conducted for the suggested value of L^d.

In 1999, the attempt to measure the localized compressive fracture length was performed by Nakamura and Higai[4]. The localized compressive fracture length was obtained by considering the local strain, which was measured by embedding a deformed acrylic bar attached with strain gages inside concrete cylinder specimens. It was found that the localization behavior can be captured effectively but the evaluation method of the localized compressive fracture length was not clearly presented and the parameters of the study mainly focused on the properties of concrete used in casting of specimens.

On the other hand, the definition of fracture energy in compression also remains uncertain. Nakamura and Higai[4] defined the local fracture energy, G_{fc}, as the absorbed energy per unit area in fracture zone. The absorbed energy in fracture zone was estimated by the area under the overall load-deformation curve excluding the elastic unloading part. The compressive fracture energy, W_q, was alternatively defined as the energy dissipated up to the point where the load descends to 1/3 of the peak load which contains a portion of the elastic strain energy as presented by Rokugo and Koyanagi[9].

Therefore, in this paper, an experimental program has been conducted in order to clarify the localized behavior of concrete in compression. The experiment is divided into 2 parts. The first part considers the wide range of geometrical parameters

Table 1 Experimental Program: Part I

(a) Experimental program

Specimen	Cross-section (mm×mm)	Height (mm)	H/D	Designation
Prism	200×200	800	4	PS20-80
		400	2	PS20-40
		200	1	PS20-20
	200×100	800	4	PR20-80
		400	2	PR20-40
		200	1	PR20-20
	100×100	400	4	PS10-40
		200	2	PS10-20
		100	1	PS10-10
Cylinder	ϕ200	800	4	C20-80
		400	2	C20-40
		200	1	C20-20
	ϕ100	400	4	C10-40
		200	2	C10-20
		100	1	C10-10

**Average cylindrical compressive strength at 7 days for all cases is 45 N/mm² with the maximum size of coarse aggregate 20 mm.*

(b) Mix proportion of concrete**

Name of Mixture	G_{max} (mm)	W/C (%)	s/a (%)	Unit weight per volume (kg/m³)				
				W	C	S	G (mm)	
							5-13	13-20
25	20	50	45	185	370	799	494	494

***No admixture was added and the air content is 2.0%.*

such as the height-depth ratio, shape and size of a specimen. The effects of the parameters on the localized compressive fracture length and fracture energy in compression of concrete under uniaxial compressive stress will be determined while the properties of concrete are kept constant.

The effects of the concrete properties, i.e. cylindrical compressive strength and maximum size of coarse aggregate on the localized compressive fracture length and fracture energy in compression have been examined subsequently in the second part. In all tests, the high early strength cement is used. Finally, the quantitative judgment of localized compressive fracture length and the definition of compressive fracture energy are introduced.

3. EXPERIMENT

(1) Part I

The effects of the geometrical parameters; the height-depth ratio, size and shape of the specimens on the failure of specimens relating to localized compressive fracture length and compressive fracture energy have been examined. The details of the experimental program are listed in **Table 1(a)**.

All specimens were cast by using the same mix

proportion of concrete with the average cylindrical compressive strength of 45 N/mm^2, and the quantities of material used are shown in **Table 1 (b)**. The tops of specimens were capped by cement paste at 6-8 hours after the casting to ensure the smooth horizontal surface while loaded. Specimens were demolded after one day and were cured in water of about 22 °C for 7 to 8 days before tested. The compressive strength tests of concrete cylinder ϕ 100 × 200 mm taken from the same batch of the specimen were also conducted.

The technique of measuring strain inside a concrete specimen by embedding a deformed acrylic resin square bar studied by Nakamura and Higai[4] was found effective and was adopted in this experiment. The acrylic resin square bar with cross-section of 10 × 10 mm, was first deformed by furrowing half cylinder-shaped gutters along the 2 opposite sides of the acrylic bar in order to ensure the good bond between the bar and concrete, as shown in **Fig.1 (a)**. Then, the deformed bar was attached by strain gages and installed vertically at the position coincident with the specimen axis before casting of concrete. The strain gages were attached to the bar vertically to measure the longitudinal local strain at the interval of 40 mm (or 20 mm in case of 100 mm height specimen). The total deformation of a specimen was externally measured by the use of deflection gages set between loading plates while the specimen was loaded in the testing machine. The reduction of the friction between the end of a concrete specimen and loading platen interfaces was done by placing friction reducing pad sets consisted of two teflon sheets inserted by silicon grease. As for the standard cylindrical compressive strength tests of the ϕ 100 × 200 mm cylinder, there was no attempt to reduce the friction between specimen ends and loading plates. The installation of the deformed acrylic bar and the test set up are illustrated in **Fig.1**. All the data were recorded through the data logger.

The post-peak load-deformation curves were captured by the one directional repeated loading in the stress descending range. The initiation and the propagation of cracks were also visually observed.

(2) Part II

In this part, only the cylinder specimens ϕ 100 × 400 mm were used throughout the testing program. A deformed acrylic bar attached with strain gages was also embedded inside all specimens. The parameters of concrete properties, i.e. the maximum size of coarse aggregate, G_{max}, and the water-cement ratio, W/C, of concrete used in casting were changed as shown in **Table 2**. The processes of preparation of a specimen are the same as in the experiment Part I, excepted that instead of capping the tops of specimens, the tops of specimens were ground.

The testing procedures were also the same as in Part I.

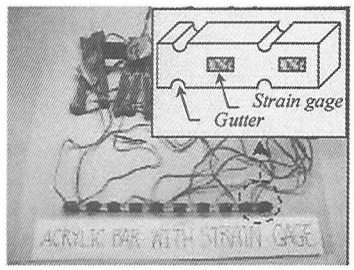

(a) Acrylic bar with strain gages

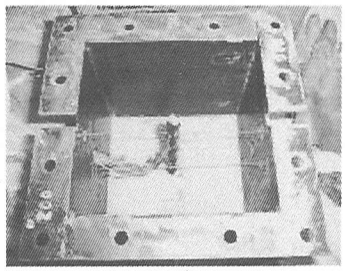

(b) Installation of acrylic bar

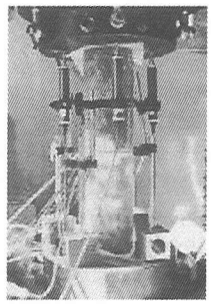

(c) Loading set up

Fig.1 The installation of strain gages and the test set up

Table 2 Experimental program: Part II*

Name of Mixture	G_{max} (mm)	W/C (%)	s/a (%)	Unit weight per volume (kg/m^3)				
				W	C	S	G (mm)	
							5-13	13-20
15	13	50	49	190	380	853	898	-
16		60	51	190	317	915	889	-
17		70	53	190	271	970	870	-
25	20	50	45	185	370	799	494	494
26		60	47	185	308	859	490	490
27		70	49	185	264	913	481	481

**No admixture was added and the air content for G_{max} 13 and 20 mm is 2.5% and 2.0%, respectively.*

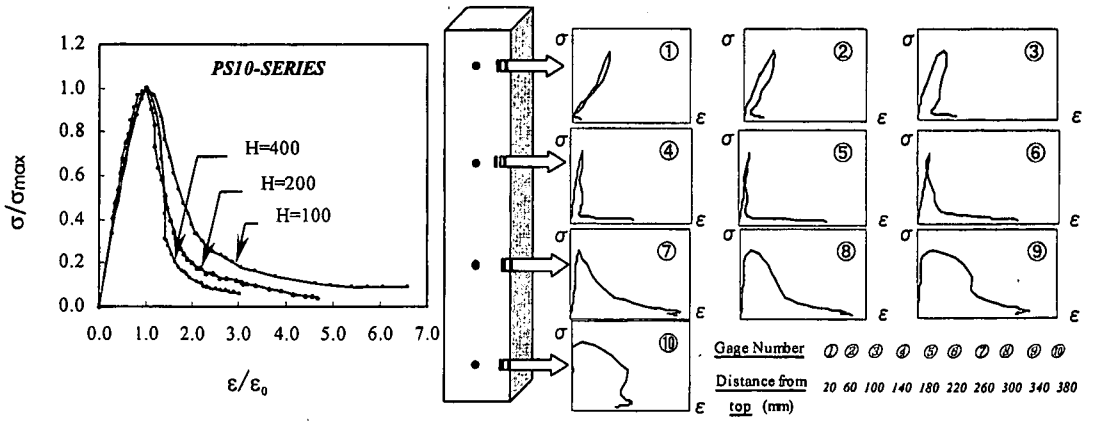

(a) Externally measured stress-strain curves (b) Local stress-strain curves (PS10-40)

Fig.2 Typical results from experiment Part I (PS10-SERIES)

4. DETERMINATION OF LOCALIZED COMPRESSIVE FRACTURE LENGTH AND FRACTURE ENERGY IN COMPRESSION

After compiling all the test results, the overall average stress-strain curves from the external measurement, together with the local stress-strain curves measured by each gage attached to the deformed acrylic bar are plotted as an example of PS10-SERIES specimens shown in the **Fig.2 (a)** and **(b)**. The σ_{max} and ε_0 refer to the maximum stress and corresponding strain, respectively.

(1) Localized compressive fracture length, L_p

It can be seen from local stress-strain curves of PS10-40 shown as in **Fig.2 (b)** (the full results with numerical values of PS10-40 are summarized in **APPENDIX A**) that, within the stress descending range, some parts of the specimen show the softening behavior (increasing of strain) while some parts show the unloading behavior (decreasing of strain). That means, in this case, failure was localized into some part of the specimen.

As cited before, many research works tried to set up the value of fracture length or the localized compressive fracture length, L_p, based on various test results. Most of them did not measure directly the value of L_p but rather theoretically set up[6], or else based on the length which believed that some part of specimen is subjected to uniform uniaxial compressive stress[5),7)]. Nevertheless, the direct measurement of the L_p, was already studied by Nakamura and Higai[4)] but the determination of L_p in their study is based on the distinction between the increasing zone of the local strain (softening zone) from the decreasing zone (unloading zone) which is, somehow, indistinctive judgment. The problem was also raised when some parts of the specimen showed unloading behavior at the beginning of the descending path, then they changed into softening behavior when the load was further applied, as can be seen from curves of gage number 3 to 6 in **Fig.2 (b)**.

For those reasons, in this paper, a newly developed concept of the determination of L_p is introduced. The energy consumed by each specimen portion calculated based the load-local deformation curve is used to be the criterion in the judgment of the L_p.

From the load-local deformation curves of a specimen, the energy consumed by the whole specimen can be calculated by summing up the energy consumed in each portion of the specimen which is assumed to have a constant strain within the interval equal to the space between strain gages as depicted in **Fig.3**. **Fig.3 (a)** shows the portion assumed to have constant strain, while **Fig.3 (b)** shows the area beneath the load-local deformation, $P\text{-}d_i$, curve up to 10% of load at the maximum resistance, P_{max}, within the descending range of that specimen portion. The calculated area, i.e. dark-shaded area, therefore, is the energy consumed within that specimen portion which will be called $A_{int,i}$. The summation of the $A_{int,i}$ yields the total energy consumed by the whole specimen or A_{int}, as shown in Eq. (1).

$$A_{int} = \sum_{i=1}^{n} A_{int,i} \qquad \text{(N-mm)} \quad (1)$$

where, n is the total number of the gages attached to the deformed acrylic bar.

Therefore, the distinct and objective definition of

the compressive fracture zone is then given as the zone in which the value of A_{inti} is larger than 15 percent of A_{int}, and the length of the zone is called localized compressive fracture length, L_p (**Fig.3 (c)**). The criterion of 15 percent is selected because the obtained results from calculation of L_p yielded the good evaluation compared with the observation from the experiments. Besides, for the portions in which A_{inti} are greater than 15 percent of A_{int}, it can be perceived that the energy absorbed by those specimen portions are considerably high enough and leaded to the failure of those portions.

(2) Compressive fracture energy, G_{Fc}

The definition of compressive fracture energy has also been suggested by many researchers. Nakamura and Higai[4] defined the local compressive fracture energy by the absorbed energy, which was caused by externally applied load up to 20% of the P_{max}, within softening range excluding the elastic unloading path, per unit area of the specimen cross-section. Whereas, Rokugo and Koyanagi[9] defined the total absorbed energy up to 1/3 (approximately 33%) of the P_{max} in the descending range as the compressive fracture energy. It can be obviously seen that the unique definition has not been set up yet. One reason may come from the lack of the reliable data on the fracture length, L_p. Hence, in this paper, based on the L_p obtained from the newly developed criterion, the G_{Fc} is evaluated from the energy consumed by the specimen up to 10% of the P_{max} within the descending range and the true fracture volume, V_p, which is considered to be damaged by the externally applied load. The concept of G_{Fc} based on the fracture volume, V_p (not the area), is introduced here since, in the realistic manner, the externally applied energy would rather cause the volumetric failure than the failure at any specific cross-section of a specimen. Additionally, the value of 10% of the P_{max} is used because, from the experiment, it was found to be the level of load in which if a specimen was further loaded, there would be only small change in the total deformation of a specimen.

In the same way as A_{inti}, the A_{ext} based on the load-overall deformation, P-d, curve measured externally can be calculated. The A_{ext} is, in other words, the total energy supplied by externally applied load which caused the failure to the specimen. The main failure part of a specimen is the localized fracture volume, V_p, which is the product of L_p and the specimen cross-sectional area, A_c. Therefore, the compressive fracture energy, G_{Fc}, which is the applied energy per unit volume of the fracture zone, can be calculated by dividing the

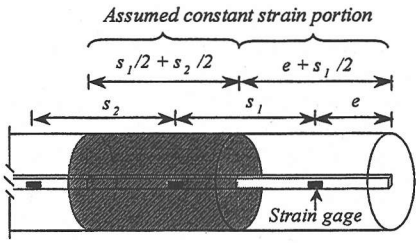

(a) Assumed length of uniform strain distribution

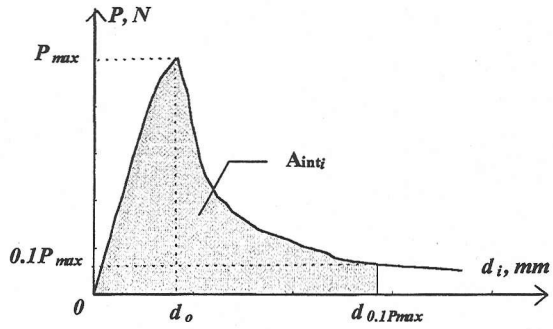

(b) Energy consumed by each portion, A_{inti} (Load-local deformation curve)

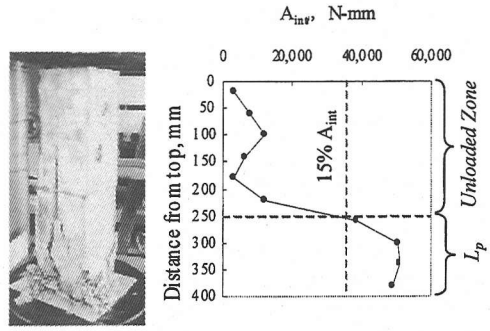

(c) Localized compressive fracture zone

Fig.3 Determination of L_p

obtained A_{ext} by V_p as shown in Eq.(2).

$$G_{Fc} = \frac{A_{ext}}{V_p} \qquad (\mathrm{N/mm^2}) \qquad (2)$$

where,

V_p = Localized fracture volume, mm^3

$= L_p \times A_c$

A_c = Concrete cross-sectional area, mm^2

The results of L_p and G_{Fc} for the experiment Part I and II are summarized in **Table 3(a)** and **(b)**, respectively.

Table 3 Summary of test results

(a) Part I

Specimen		Section (mm)	A_C (mm^2)	H (mm)	H/D	σ_{max} (N/mm^2)	f_c' (N/mm^2)	σ_{max}/f_c' (%)	L_p (mm)	G_{Fc} (N/mm^2)
PRISM	PS20-80	200×200	40,000	800	4	30.1	47.5	63.3	120	0.694
	PS20-40			400	2	29.7	43.5	68.3	90	0.462
	PS20-20			200	1	23.7	39.6	59.8	160	0.165
	PR20-80	200×100	20,000	800	4*	30.5	39.4	77.2	220	0.530
	PR20-40			400	2*	35.7	43.5	82.1	150	0.238
	PR20-20			200	1*	37.6	50.4	74.6	200	0.176
	PS10-40	100×100	10,000	400	4	30.5	46.7	65.4	145	0.216
	PS10-20			200	2	39.4	50.4	58.2	130	0.182
	PS10-10			100	1	25.7	47.3	54.3	50	0.188
CYLINDER	C20-80	φ200	31,416	800	4	34.3	47.5	72.3	130	0.352
	C20-40			400	2	28.1	43.5	64.6	95	0.386
	C20-20			200	1	22.5	50.4	44.6	160	0.150
	C10-40	φ100	7,854	400	4	30.5	45.6	66.9	135	0.189
	C10-20			200	2	31.2	39.9	78.1	120	0.206
	C10-10			100	1	20.0	39.6	50.5	100	**

**For PR20-SERIES, D = 200 mm was used.*

*** Result not available.*

(b) Part II

Cross-section×Length (mm)	Maximum size of aggregate (mm)	Water-cement ratio	σ_{max} (N/mm^2)	f_c' (N/mm^2)	σ_{max}/f_c' (%)	L_p (mm)	G_{Fc} (N/mm^2)
Cylinder φ100×400	*20*	0.50	32.5	45.7	71.1	115	0.215
		0.60	30.4	36.7	82.8	110	0.239
		0.70	22.6	28.4	79.6	148	0.186
	13	0.50	39.4	46.4	84.9	120	0.261
		0.60	29.4	32.2	91.3	118	0.225
		0.70	21.8	26.2	83.3	125	0.178

5. CRACKING PATTERNS

Many researchers have reported the effects of end restrain on the measured stress-strain curve of concrete under uniaxial compression[3), 8), 10)]. Thus, as mentioned above, in all tests here, the attempt to reduce the friction between the specimen ends and loading platens was done by the use of friction-reducing pads. From the test results shown in **Table 3(a)** and **(b)**, the ratios of the maximum stress of the specimen to its cylindrical compressive strength, σ_{max}/f_c', are changing. However, the average values are 71% and 76% when H/D=2 and 4, respectively, which means the friction was effectively removed by the friction-reducing pads.

In the case of H/D = 1, the average σ_{max}/f_c' is 57%. The reason why this low value is obtained is because specimens with H/D=1 failed in the splitting failure mode, which is completely different from the cases when H/D≥2.

Moreover, from the observation of cracks, it was found that, for specimen with H/D≥2, failure did not commence at the central zone of a specimen but was initiated from either end of a specimen, that means the effects of end restrain was substantially eliminated. The additional reason is because of the fact that, the nature of the concrete is inhomogeneous and the strength of the concrete throughout the length is subjected to normally distributed variation, hence stabilized failure throughout the length cannot be expected. Furthermore, due to some unavoidable imperfections of the testing conditions, such as the horizontality of the loading plate, the perfect uniform force transferability from the both ends throughout the length is unlikely to be occurred, especially when the length of the specimen increases; therefore the failure is tentatively to be initiated from either end of the specimen.

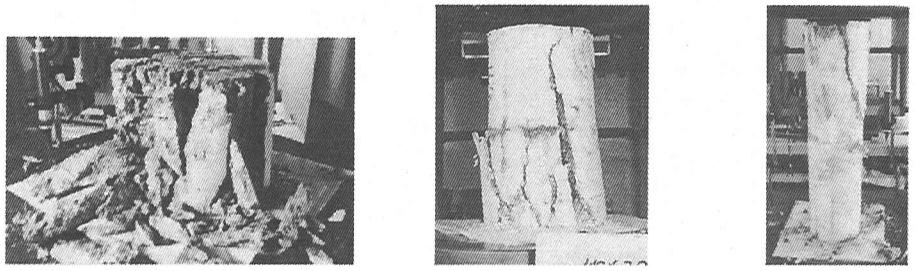

(a) H/D=1 (b) H/D=2 (c) H/D=4

Fig.4 Cracking patterns of tested specimens (C10-SERIES) (experiment Part I)

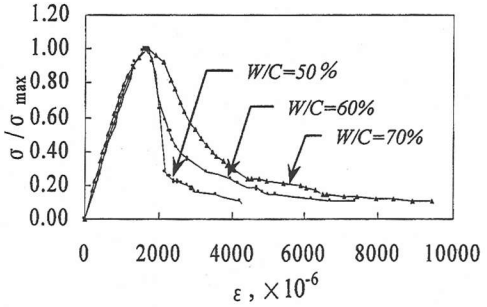

Fig.5 Typical results from experiment Part II (G_{max} = 20 mm)

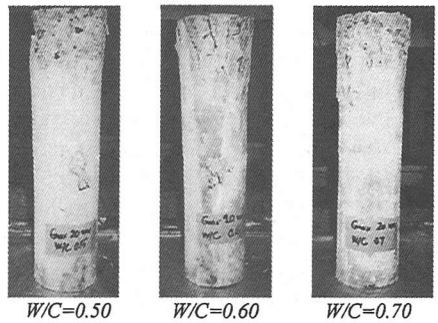

(a) G_{max} = 20 mm

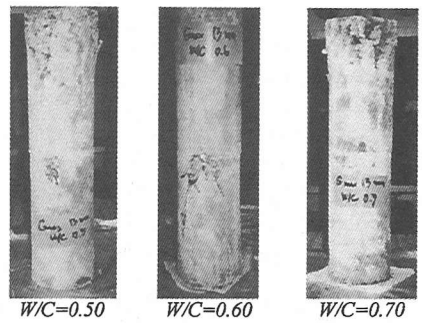

(b) G_{max} = 13 mm

Fig.6 Cracking patterns of tested specimens (experiment Part II)

(1) Experiment Part I

From the observation of the occurrence of cracks on tested specimens, it can be seen that, for the short specimens with H/D=1, specimens were failed by the splitting from the top to the bottom of a specimen and the observed value of compressive fracture length, L_p, are, almost in all cases, equal to H. As for the longer specimen, H/D=2 and 4, lots of small visible vertical cracks were observed over some regions when the peak resistance was reached. At the final stage, in the post peak region at $0.1P_{max}$, the small cracks were coalesced forming the crack zone accompanied with few long vertical cracks penetrated down to the bottom part of specimens (in case specimens failed from top). That means the localization occurred just in the case of H/D≥2, hence the later sections discussing about L_p and G_{Fc} will refer to only the results of specimens having H/D≥2. This localization behavior can also be clearly seen from the cracking pattern of the specimen at the final stage shown in **Fig.4.**

It should be noted that, compared with the work done by Markeset[5], this vertical cracks are supposed to be localized into a shear band but positioned vertically in this experiment because the friction at both ends were effectively removed.

(2) Experiment Part II

The further observation on the effects of the maximum size of coarse aggregate and the water-cement ratio of concrete used in the casting of a specimen on the localization in compression has been carried out. The concrete cylinder specimens with diameter of 100 mm and the height of 400 mm were selected and tested. The typical results are depicted in **Fig.5.**

From **Fig.6 (a), (b)** and from the observation of cracks during the tests, it can be seen that the localization occurred in some part of a specimen with few penetrating long cracks as in the experiment Part I. There is no significant difference in cracking patterns when specimens have different concrete properties.

It is of an interesting to be noticed that the slope of each local stress-strain curve shown in **Fig.2 (b)** (refer to also **APPENDIX A**) are different. The possible reason is that, when the loading was applied, the volume of the specimen started to be decreasing by the shortening of the length, then followed by the occurrence of the lateral expansion. However, due to the residual frictional restraint at both ends of the specimen, although the attempt to remove it had been proceeded, and because of the inhomogeneity of concrete itself, the expansion of the top and the bottom portion were different. In this case, PS10-40 (**Fig.3 (c)**), the bottom expansion seemed to be larger than at the top, while the top portion showed greater in the shortening of the length, i.e. not yet expanded. Therefore, the ascending curves of the local gages positioned within the upper portion of the specimen, showed the significant change in longitudinal strain, whereas the lower portion, especially gage 10, showed only a slightly change as can be seen from **Fig.2 (b)**. On the other hand, after the peak load, the lower portion in which the expansion is greater than the upper portion, failed at the final state, in other words, failure localized at the bottom. This also confirms the concept that within the localized failure zone, most of the applied energy were consumed, as can be seen from area under the local strain curves, i.e. the higher A_{int} of the gages positioned at the lower part was observed compared with the upper ones.

In the conclusion from the test results, in all cases, they have shown that for specimens whose length greater than L_p, the final failure pattern is the combination of few long penetrating cracks and a zone containing lots of small splitting cracks. The penetrating crack is, in general, the diagonal shear band, but in this study the frictional restraint at both ends of the specimens has been removed during the tests, therefore the deviation of the crack inclination from the vertical direction is relatively small. For the zone containing splitting cracks, which indicated the volumetric failure, it contributed to the failure to most of the specimen; as a result, in this research, the determination of L_p is based on the length of this zone. Accordingly, G_{Fc}, which is defined as the energy required to cause compressive failure to a unit volume of the specimen, can then be calculated based on the externally applied energy and the localized failure volume, i.e. the zone containing splitting cracks, as described in details in the sections 6 and 7.

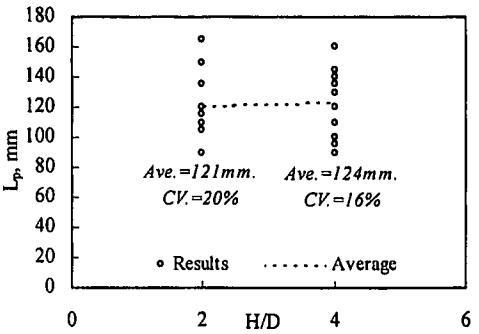

Fig.7 The variation of L_p with the H/D ratio

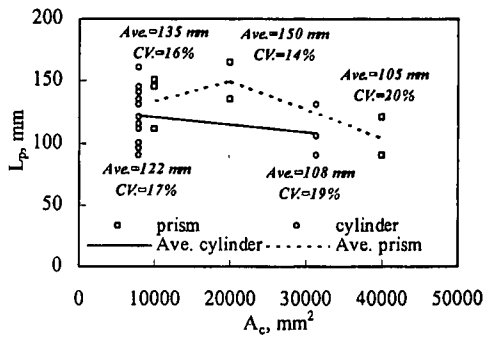

Fig.8 The variation of L_p with the cross-section size and shape of specimens

6. LOCALIZED COMPRESSIVE FRACTURE LENGTH, L_p

(1) Effects of geometrical parameters

The effects of each geometrical parameters are discussed, excluding the case of H/D=1, as the followings.

a) Height-depth ratio

By including also the results from the experiment Part II, **Fig.7** shows that the variation of H/D of a specimen causes no significant change to L_p. The average value of L_p almost equal to 120 mm was obtained for both H/D=2 and 4 cases. In other words, the change in height of a specimen of the same cross section has no significant effects on L_p. The results of PR20-80 were excluded from the consideration because at the final stage a long big penetrating crack from the top down to the bottom was observed, which showed that the specimen failed in different failure mode.

b) Size and shape of specimen

From **Fig.8**, it can be further observed that, for a specimen having the same type of cross-section, the

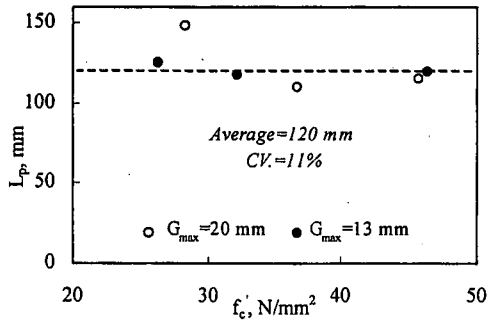

Fig.9 The relationship between L_p and concrete cylinder compressive strength

increase in the cross-sectional area leads to the slight decrease in L_p while the square and rectangular cross-section specimens show a bit slightly higher values of L_p compared with cylinder specimens.

(2) Effects of concrete properties

From the experiments, the relationship between the obtained localized compressive fracture length and the cylindrical compressive strength can be plotted as shown in **Fig.9**.

It can be seen that, regardless of the f_c' and G_{max}, almost constant L_p is obtained with the average value of 120 mm and the coefficient of variation of 11%. That means, compared with geometrical parameters, the G_{max} and W/C have small effects on the localized compressive fracture length of the specimen.

(3) Formulation of L_p

As it was found that the height and shape of a specimen and also the properties of concrete used in casting specimens have virtually small effects on L_p, whereas L_p is found to be evidently dependent on the cross-sectional area of a specimen. Therefore, the relation between L_p and the size of cross-section of a specimen in terms of D^*, the equivalent cross-section width which is the square root of the cross-sectional area, A_c, has been considered. The plot between concrete cross-sectional area and L_p/D^* in **Fig.10 (a)** shows that, within the range of the test, the almost constant value of L_p/D^* can be observed when D^* is less than 100 mm (A_c<10,000 mm^2). The increase in A_c leads to the decrease in L_p/D^* in which the rate of decreasing is gradually reduced. In order to simplify the relationship, the constant value of L_p/D^* when D^* larger than 180 mm (A_c>32,400 mm^2) was assumed.

Finally, the following simplified relationship can be proposed,

$$\begin{aligned} L_p/D^* &= 1.36 && ; \ D^*<100 \\ &= -3.53\times10^{-5}D^{*2}+1.71 && ; \ 100\le D^*\le 180 \\ &= 0.57 && ; \ D^*>180 \end{aligned} \quad (3)$$

(mm)

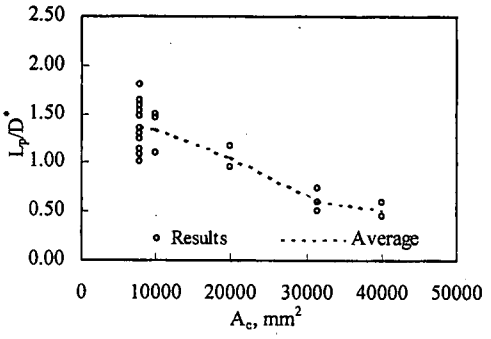

(a) Experimental results

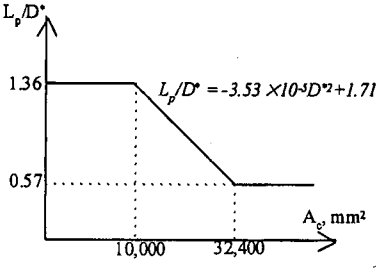

(b) Proposed formulation

Fig.10 Relation of L_p and equivalent width of the specimen

where,

$$D^* = \sqrt{A_C}\ , \text{mm}$$

or, as depicted in **Fig.10 (b)**.

The effects of various parameters of concrete specimens on the L_p, which was obtained from the direct measurement, were also studied by Nakamura and Higai[4]. The uniaxial compressive tests on concrete cylinders of ϕ 100 and ϕ 150 mm with a range of H/D ratios were performed. It was found that, the H/D ratios have less effect on L_p which confirms the test results of this study. However, the results of their study further showed that the cross-sectional area of specimens have no effects on L_p, while L_p rather effected by the f_c' and size and grading of aggregates. This may be because of the narrower range of the tested specimens cross-sectional area in their test. In addition, the determination of L_p is not quantitatively evaluated, which is different from the criterion presented here. On the contrary, according to the experimental research done by Rokugo and Koyanagi[9], it was found that L_p tends to be constant for the concrete specimens with the same cross-sectional area.

7. COMPRESSIVE FRACTURE ENERGY, G_{Fc}

As mentioned earlier, the one directional repeated loading in the stress descending range was conducted in order to capture the stress-strain curve within the post-peak region. However, for the specimens with comparatively large cross-section, the sudden drop of the load when the peak point within the descending range was reached, somehow, unavoidably occurred. Furthermore, G_{Fc} is substantially dependent on the area under the load-overall deformation curve or the shape of the curve, especially the descending range, itself. Therefore, in order to gain the most reliable tendency, the results of the C20 and PS20 series were not included in the consideration of G_{Fc}, and then **Fig.11** was plotted.

(1) Effects of geometrical parameters

Fig.11 (a) shows the relationship between the total specimen volume, V_c, and the average value of G_{Fc} of the cylinder and prism specimens. In order to consider only the effects of the geometrical parameters, the results of experiment Part II were not included. It can be seen that there was almost no change of the G_{Fc} with the change in geometry of specimens.

(2) Effects of concrete properties

Fig.11 (b) shows that the value of G_{Fc} is, in some way, dependent on the cylindrical compressive strength. It is found that when G_{Fc} was divided by $f_c'^{1/4}$, the almost constant average value of 0.86×10^{-1} with the coefficient of variation of 18% was obtained, as shown in **Fig.11 (c)**.

On the other hand, from **Fig.12** it can be seen that the maximum size of coarse aggregate has small effects on the magnitude of G_{Fc}.

(3) Formulation of G_{Fc}

Hence, from **Fig.11(c)**, when the localization in compression occurs, the following simplified relationship can be obtained,

$$G_{Fc} = 0.86\times10^{-1} f_c'^{1/4} \qquad (4)$$

where, the unit of G_{Fc} and f_c' is N/mm^2.

The obtained formulation is consistent with the previous research work[4] that the fracture energy in compression depended on concrete compressive strength regardless of the size and shape of the concrete specimen. Though the formulation is different because of the difference in the definition of the G_{Fc} but it can be conceived that the relation between G_{Fc} and f_c' is nonlinear.

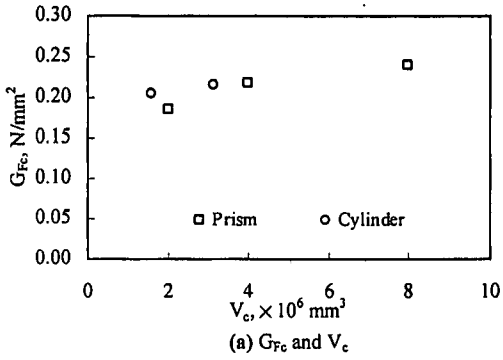

(a) G_{Fc} and V_c

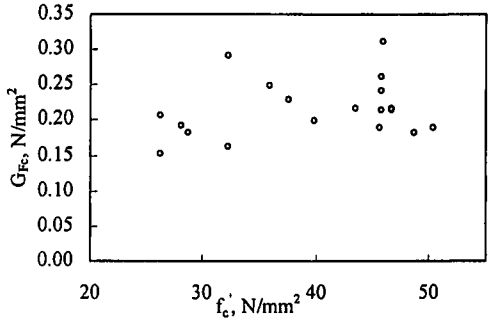

(b) G_{Fc} and f_c'

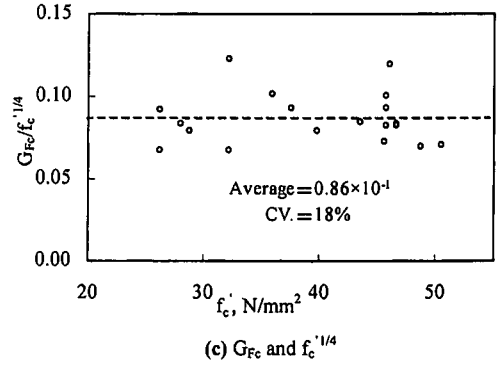

(c) G_{Fc} and $f_c'^{1/4}$

Fig.11 Relationship of G_{Fc} and parameters in the tests

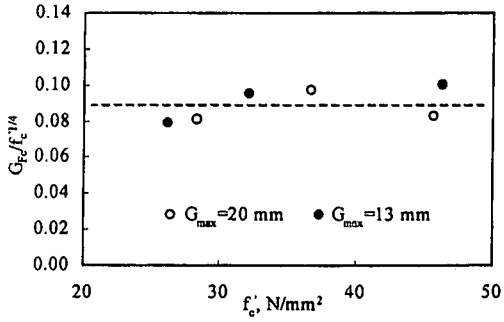

Fig.12 The relationship between G_{Fc} and f_c'

However, the actual cracking pattern of the concrete specimen is composed of the zone containing lots of small cracks, and a small number of penetrating long cracks. The calculation of G_{Fc} here based on only the small cracking zone, which is simulated by the localized fracture volume, while the long penetrating cracks and the unloading portion which consumed some parts of the external applied energy were not taken into consideration. Noted that the results of PR20-80 was also not included here because the final failure pattern of the specimen, which consisted of a long and widely open splitting crack penetrating from the top to the bottom of the specimen and only few small tensile splitting cracks, is considerably different from the other specimens.

8. CONCLUDING REMARKS

By utilizing the technique of measuring the local strain inside concrete specimen along the specimen axis, it is found that the localization of the failure in uniaxial compression occurs when the concrete specimens have H/D ratio greater than or equal to 2. The localized compressive fracture length can then be evaluated based on the relative extent of the energy absorbed by each specimen portion. The method of evaluation of L_p presented here offers a new quantitative mean to determine the value of L_p and the obtained results are found to agree with the inspection during the testing procedure.

The localized compressive fracture length is found to be dependent solely on the size of the specimen cross-section, whereas the specimen height, H/D ratio and shape of the cross-section are found to have less effect on L_p. The concrete cylindrical compressive strength and the maximum size of aggregate used in casting of the specimens are found to have virtually small effects on localized compressive fracture length as well. The relation between L_p and the equivalent section width is proposed.

Subsequently, the fracture energy in compression is calculated by dividing the area under load-overall deformation by the fracture volume. The concept is different from the previous research works in which most of them were not taken into account the effect of the localized failure zone. The test results indicated that G_{Fc} varied with the change in the concrete cylindrical compressive strength while the change in geometry of specimen and the maximum size of aggregate used in casting have less effects on G_{Fc}. The relation between G_{Fc} and f_c' has been proposed.

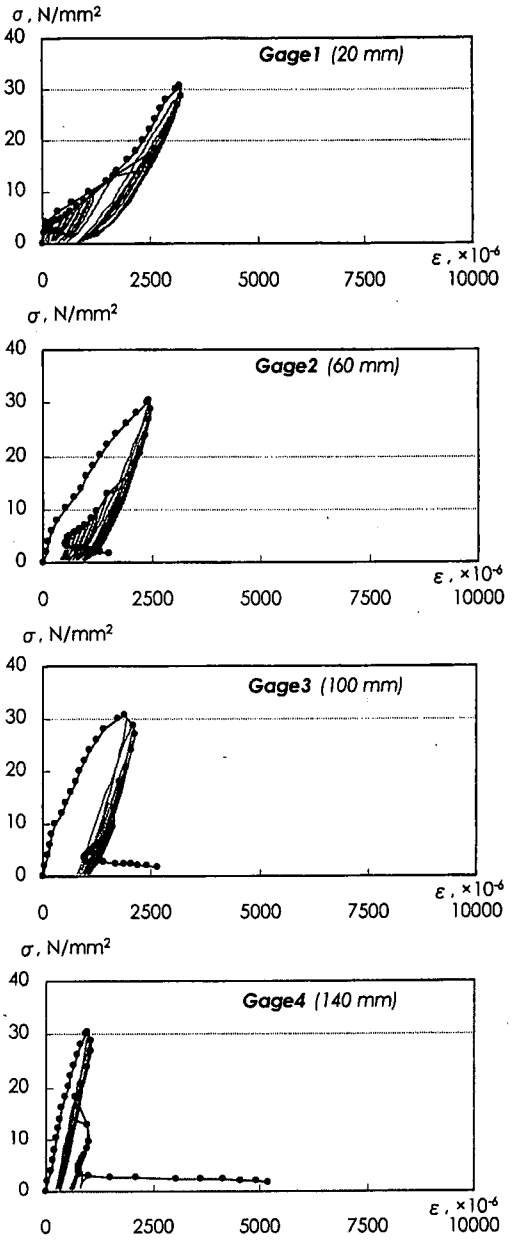

Fig.A1 Results of PS10-40 (Gage 1-4)

However, the obtained G_{Fc} did not consider the contributions from the penetrating cracks and the unloading portion which should be consequently studied in order to gain the better understanding in localization behavior in compression.

APPENDIX A TEST RESULTS OF PS10-40

The applied stress-local strain curves of PS10-40 are depicted in details in **Fig.A1**. Each curve shows

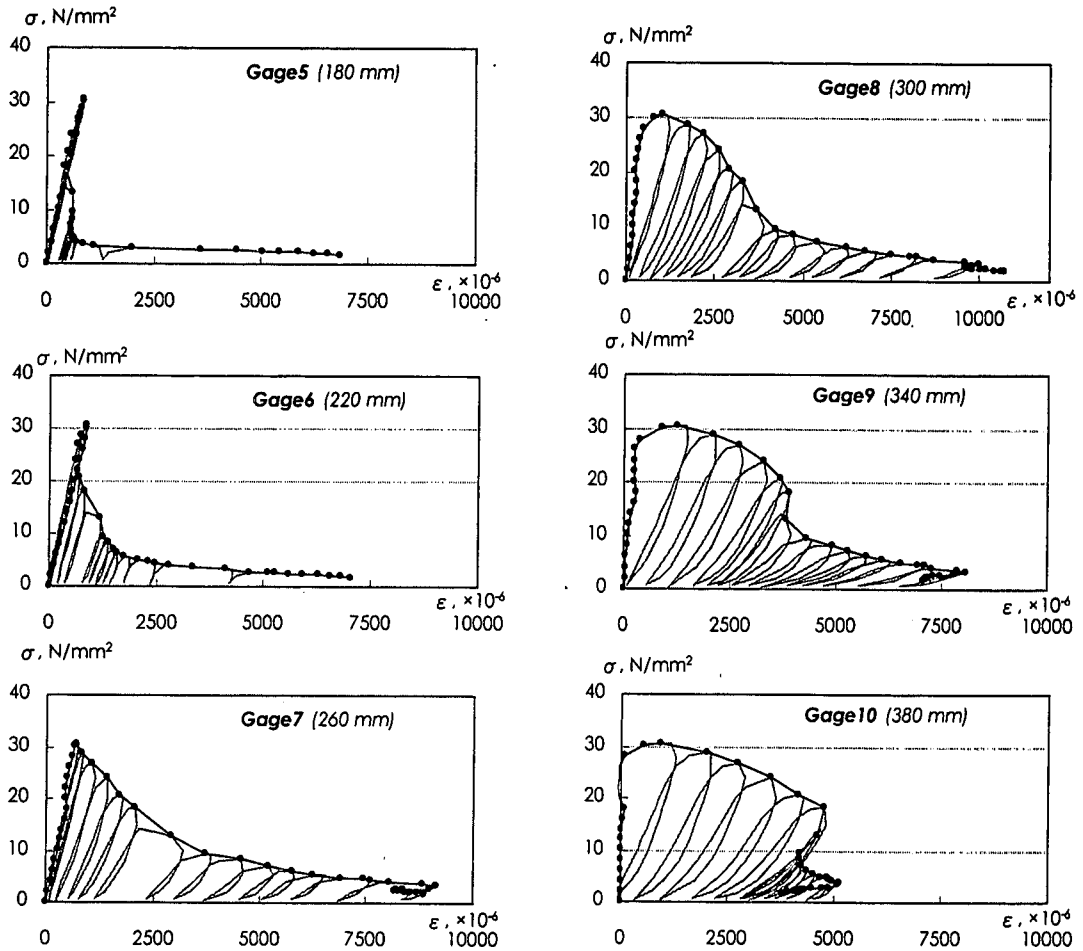

Fig.A1 Results of PS10-40 (Gage 5-10) (continued)

the path obtained from the one directional repeated loading in the stress descending range, together with the envelop curve which was achieved by connecting the peak points of the repeated curve.

APPENDIX B THE USE OF ACRYLIC BAR

The effectiveness of the local strain measurement by the deformed acrylic bar has been investigated by comparing the deformation measured externally by deflection gages, and the accumulated calculated deformation from the local strain gages throughout the whole length of specimen. It was found that the results agreed with each other well until the peak load was reached. After the peak load, the calculated deformation from local strain gages was slightly smaller than that of deflection gages as shown in **Fig.B1**. It is because, once the maximum resistance was reached, the cracks took place in the specimen,

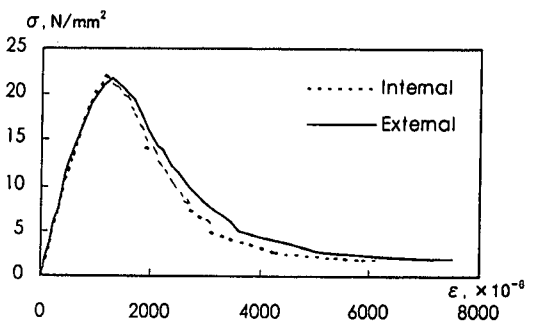

Fig.B1 Comparison between the externally (deflection gages) and internally (local strain gages) measured strain (ϕ 100×400, G_{max}=13 mm, W/C=70%)

the deflection gages continued measuring the overall-averaged deformation, whereas the calculated deformation from local strain gages is, somehow, evaluated based on the magnitude of the strain measured at the point where the strain gages located and referred as the average figure for the

interval of that gage. Anyway, the difference is negligibly small and insignificant, therefore the use of the deformed acrylic bar together with the attached strain gages to measure the internal local strain is considered reliable.

REFERENCES

1) Bažant, Z. P. and Oh, B. H.: Crack Band Theory for Fracture of Concrete, *Materials and Structures*, Vol. 16, No.93, pp. 155-177, 1983.
2) Santiago, S. D. and Hilsdorf, H. K.: Fracture Mechanisms of Concrete under Compressive Loads, *Cement and Concrete Research*, Vol. 3, pp. 363-388, 1973.
3) Sangha, C.M. and Dhir, R.K.: Strength and Complete Stress-strain Relationships for Concrete Tested in Uniaxial Compression under Different Test Conditions, *RILEM, Materiaux et Constructions*, Vol. 5, pp. 361-370, 1972.
4) Nakamura, H. and Higai, T.: Compressive Fracture Energy and Fracture Zone Length of Concrete, *JCI-C51E Seminar on Post-Peak Behavior of RC Structures Subjected to Seismic Loads*, Vol. 2, pp. 259-272, Oct. 1999.
5) Markeset, G.: Failure of Concrete under Compressive Strain Gradients, *Dr.Ing thesis 1993:110*, Norwegian Institute of Technology, Trondheim, 1993.
6) Hillerborg, A.: Fracture Mechanics Concepts Applied to Moment Capacity and Rotational Capacity of Reinforced Concrete Beams, *Engineering Fracture Mechanics*, Vol. 35, No. 1/2/3, pp. 223-240, 1990.
7) Markeset, G. and Hillerborg, A.: Softening of Concrete in Compression – Localization and Size Effects, *Cement and Concrete Research*, Vol. 25, No. 4, pp. 702-708, 1995.
8) Newman, K. and Lachance, L.: The Testing of Brittle Materials under Uniform Uniaxial Compression Stress, *Proc. ASTM*, Vol. 64, pp. 1044-1067, 1964.
9) Rokugo, K. and Koyanagi, W.: Role of Compressive Fracture Energy of Concrete on the Failure Behavior of Reinforced Concrete Beams, *in Applications of Fracture Mechanics to Reinforced Concrete (ed. A. Carpinteri)*, Elsevier applied Science, pp. 437-464, 1992.
10) Kotsovos, M.D.: Effect of Testing Techniques on the Post-Ultimate Behaviour of Concrete in Compression, , *RILEM Materials and Structures*, Vol. 16, No. 91, pp. 3-12, 1983.

(Received May 17, 2000)

圧縮を受けるコンクリートの局所化パラメータに関する実験的研究

Torsak LERTSRISAKULRAT・渡辺　健・松尾真紀・二羽淳一郎

一軸圧縮応力が作用するコンクリートの破壊メカニズムと局所化の影響について，実験的に検討した．コンクリートの軸方向局所ひずみ分布を，コンクリート供試体内部に埋め込んだひずみゲージによって測定した．そして，供試体形状やコンクリートの特性を考慮して，局所圧縮破壊長さを決定し，それに基づいてコンクリートの圧縮破壊エネルギーを提案した．本実験の結果から，圧縮破壊の局所化が生じる場合，局所圧縮破壊長さは供試体断面の大きさのみに依存し，また圧縮破壊エネルギーはコンクリート強度に左右されることを明らかにした．